UCSF
UC San Francisco Previously Published Works

Title

Unbound Corneocyte Lipid Envelopes in 12R-Lipoxygenase Deficiency Support a Specific Role in Lipid-Protein Cross-Linking

Permalink

https://escholarship.org/uc/item/4576254t

Journal

American Journal Of Pathology, 191(5)

ISSN

0002-9440

Authors

Meyer, Jason M
Crumrine, Debra
Schneider, Holm
et al.

Publication Date

2021-05-01

DOI

10.1016/j.ajpath.2021.02.005

Peer reviewed

MOLECULAR PATHOGENESIS OF GENETIC AND INHERITED DISEASES

Unbound Corneocyte Lipid Envelopes in 12R-Lipoxygenase Deficiency Support a Specific Role in Lipid-Protein Cross-Linking

Jason M. Meyer,[*] Debra Crumrine,[†] Holm Schneider,[‡] Angela Dick,[‡] Matthias Schmuth,[§] Robert Gruber,[§] Franz P.W. Radner,[¶] Susanne Grond,[¶] Joan S. Wakefield,[*] Theodora M. Mauro,[*] and Peter M. Elias[*]

From the San Francisco Veterans Affairs Medical Center, Dermatology Service[*] and UC San Francisco Department of Dermatology, San Francisco, California; the San Francisco Veterans Affairs Medical Center,[†] Dermatology Service, San Francisco, California; the Department of Pediatrics,[‡] University of Erlangen-Nürnberg, Nürnberg, Germany; the Department of Dermatology, Venereology and Allergology,[§] Medical University of Innsbruck, Innsbruck, Austria; and the Institute of Molecular Biosciences,[¶] University of Graz, Graz, Austria

Loss-of-function mutations in arachidonate lipoxygenase 12B (*ALOX12B*) are an important cause of autosomal recessive congenital ichthyosis (ARCI). 12R-lipoxygenase (12R-LOX), the protein product of *ALOX12B*, has been proposed to covalently bind the corneocyte lipid envelope (CLE) to the proteinaceous corneocyte envelope, thereby providing a scaffold for the assembly of barrier-providing, mature lipid lamellae. To test this hypothesis, an in-depth ultrastructural examination of CLEs was performed in *ALOX12B*$^{-/-}$ human and *Alox12b*$^{-/-}$ mouse epidermis, extracting samples with pyridine to distinguish covalently attached CLEs from unbound (ie, noncovalently bound) CLEs. *ALOX12B*$^{-/-}$ stratum corneum contained abundant pyridine-extractable (ie, unbound) CLEs, compared with normal stratum corneum. These unbound CLEs were associated with defective post-secretory lipid processing, and were specific to 12R-LOX deficiency, because they were not observed with deficiency of the related ARCI-associated proteins, patatin-like phospholipase 1 (*Pnpla1*) or abhydrolase domain containing 5 (*Abhd5*). These results suggest that 12R-LOX contributes specifically to CLE—corneocyte envelope cross-linking, which appears to be a prerequisite for post-secretory lipid processing, and provide insights into the pathogenesis of 12R-LOX deficiency in this subtype of ARCI, as well as other conditions that display a defective CLE. (*Am J Pathol 2021, 191: 921—929; https://doi.org/10.1016/j.ajpath.2021.02.005*)

The corneocyte lipid envelope (CLE) (Figure 1D) is a lipid membrane composed of ω-hydroxy ceramides and ω-hydroxy fatty acids that are covalently bound to the extracellular surface of the proteinaceous corneocyte envelope (CE).[1,2] Investigation of autosomal recessive congenital ichthyosis (ARCI), caused by mutations in enzymes that contribute to CLE and CE synthesis, has revealed that the CLE-CE complex is required for skin barrier function.[3–6] Altered CLE-CE composition and structure are also associated with barrier dysfunction in many other skin conditions, including atopic dermatitis[7] and psoriasis.[8]

The major unbound lipid precursor of the CLE is most likely esterified ω-hydroxy-acyl sphingosine (EOS; an abundant ω-*O*-acyl ceramide in mammalian epidermis). In the current model (Figure 1A), the final step of EOS

synthesis is transfer of linoleate (C18:2) from triglyceride to ω-hydroxy-acyl sphingosine (the ceramide ω-hydroxy-acyl sphingosine), catalyzed by patatin-like phospholipase 1 (PNPLA1) and its coactivator abhydrolase domain containing 5 (ABHD5)/comparative gene identification-58

(CGI-58).[4,9–11] EOS and glucosylated EOS are then stored and transported in lamellar bodies,[12] whose limiting membranes fuse with the plasma membrane during lipid secretion in the outer stratum granulosum at the site of the developing CLE.[5] Subsequently, oxidation reactions catalyzed sequentially by 12R-lipoxygenase (12R-LOX; encoded by the gene *ALOX12B*), epidermal lipoxygenase 3 (encoded by *ALOXE3*), and short-chain dehydrogenase/ reductase family 9C member 7 (SDR9C7) are proposed to transform the pentadiene group in the ω-linoleate of EOS into an epoxy enone that can react nonenzymatically with peptides on the external face of the CE (especially involucrin, envoplakin, and periplakin[13]) to form protein-bound ω-hydroxy-acyl sphingosine.[14,15] The bound ω-hydroxy fatty acids could be formed either by a similar sequence starting with ω-*O*-acyl fatty acids instead of EOS[16] or via hydrolysis of the amide bond of bound ω-hydroxy-acyl sphingosine by ceramidases.[17]

This model explains why both CLEs and their ω-hydroxy ceramide and ω-hydroxy fatty acid constituents are diminished in ARCI with defects in EOS synthesis[4,5] or EOS oxidation. The phenotype associated with these two subgroups of ARCI is indistinguishable,[18] consistent with the possibility that the disease features are a consequence of the shared CLE defect. However, one major difference is that unbound EOS is reduced in EOS synthesis defects, but normal or increased in EOS oxidation defects (the metabolic changes associated with these differences are illustrated) (Supplemental Figure S1).[19,20] Some of this excess EOS could be contained within abnormal CLEs that fail to be cross-linked to protein (referred to as unbound CLEs throughout this article) due to the defect in EOS oxidation, although these have not yet been reported. The identification of such unbound CLEs would support a specific role for 12R-LOX in CLE-CE cross-linking and could provide insight into CLE biogenesis and the potential treatment of CLE defects in ichthyosis and other conditions. Therefore, in the current study, a detailed ultrastructural examination was performed on epidermis from an *ALOX12B*^{−/−} ARCI patient and from *Alox12b*^{−/−} mice, using the amphipathic solvent pyridine to distinguish unbound from bound CLEs.

Materials and Methods

Human Subject Skin Samples and Animal Models

The ARCI skin sample was collected at the Medical University of Innsbruck from the chest of a 53-year−old man with congenital ichthyosis under an ethics board approved human subject research protocol (number AN 2049, Skin Barrier: Consequences of Defined Mutations in Structural and Functional Proteins). Additional clinical information about this patient is given in *Results*, Figure 1, and Supplemental Figure S2. The unaffected skin sample was from normal-appearing skin that was collected from discarded tissue during a skin cancer excision at the San

Francisco Veterans Affairs Medical Center. Tamoxifen-inducible keratinocyte-specific *Alox12b* conditional knockout mice,[19] *Pnpla1* knockout mice,[21] and keratinocyte-specific *Abhd5* knockout mice[21] were previously described, and loss of expression of the gene of interest was confirmed in each model. For simplicity, these mice are designated wild type or +/+ and knockout or −/− in the text and figures, although the controls in the conditional knockout mice (*Alox12b* and *Abhd5*) have the gene of interest flanked by engineered locus of crossover in P1 sites. The *Alox12b* conditional knockout mice developed diffuse erythema and scale in the first week after starting tamoxifen injections, and biopsy samples were from adult mice on day 8 after starting tamoxifen injections. The *Pnpla1* and keratinocyte-specific *Abhd5* knockout mice were born with barrier failure and hyperkeratosis, and biopsy samples were from neonatal mice. Epidermis from a neonatal mouse with constitutive deletion of *Alox12b* (described previously[14]) was also examined and was not significantly different from the adult, conditional *Alox12b* knockout mice (data not shown). Examination and analysis were done on samples from one mouse chosen randomly from the three available for each genotype, and the major findings presented in the figures were confirmed by examination of samples from a second, randomly selected mouse from each group.

Electron Microscopy

For standard electron microscopy, skin samples were minced into fragments <0.5 mm^3, prefixed in half-strength Karnovsky's fixative, rinsed three times in 0.1 mol/L cacodylate buffer, followed by post-fixation in reduced osmium tetroxide or ruthenium tetroxide (Polysciences, Warrington, PA), as indicated in the figure legends. Samples were then embedded in epoxy-Epon (Hexion, Columbus, OH) and processed for electron microscopy, as described.[22] To examine bound lipids (including the CLE), skin samples were flash frozen after collection, thawed in absolute pyridine for 2 hours at room temperature,[1] rinsed in 0.1 mol/L cacodylate buffer, and post-fixed with reduced osmium tetroxide before embedding in epoxy-Epon. Imaging was done on thin sections using a JEOL (Peabody, MA) 100CX electron microscope at 60 V with a Gatan (Pleasanton, CA) Bioscan camera (model 792).

Image Analysis and Quantification

Images in the figures are representative of the entire sample. CLE abundance was quantified on 10 random (selected using blinded movements of the microscope stage), high-magnification fields in the mid−stratum corneum (SC) by measuring the length of CLE-CE complex in each field and dividing this by the total CE length in the field. CLE abundance values are expressed as a percentage of the value obtained with pyridine-extracted samples of normal skin from an unaffected human subject or from wild-type control mice, to control for differences between separate sample
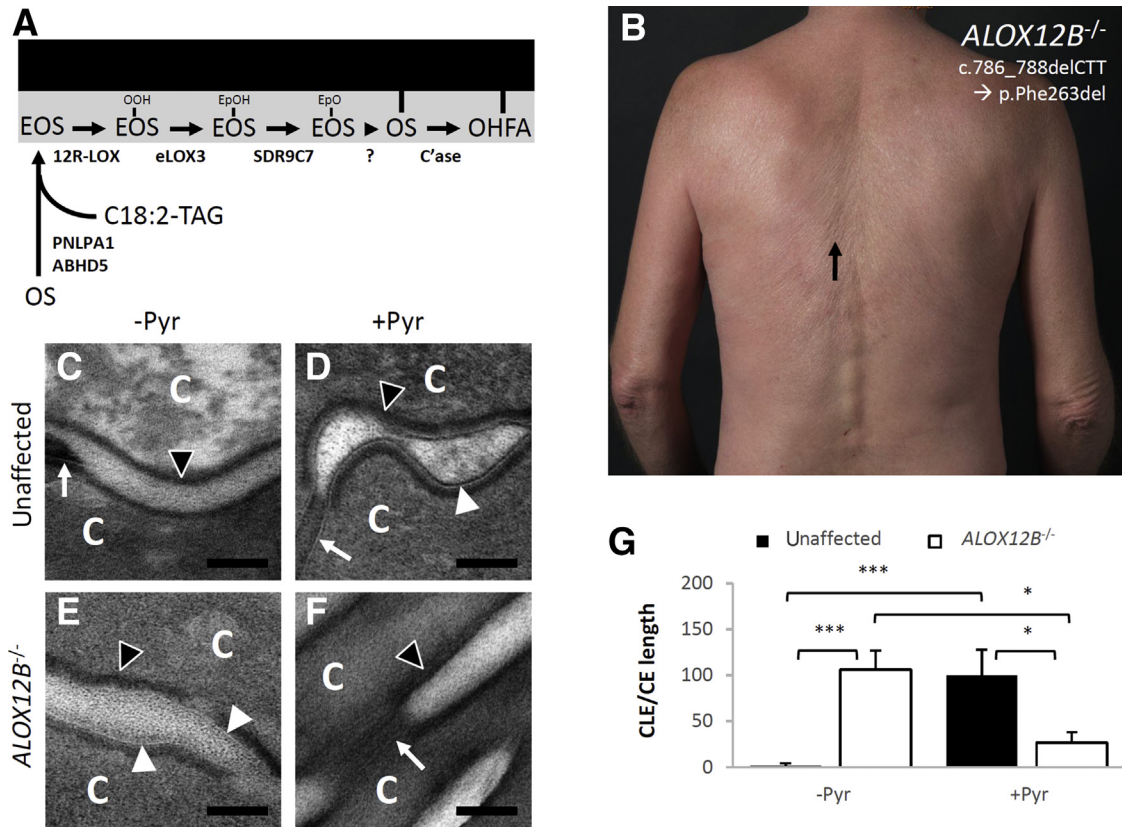
Figure 1 Unbound corneocyte lipid envelopes (CLEs) in *ALOX12B*$^{-/-}$ autosomal recessive congenital ichthyosis (ARCI). **A:** The current model of CLE biogenesis involves esterified ω-hydroxy-acyl sphingosine (EOS) synthesis catalyzed by patatin-like phospholipase 1 (PNPLA1) and abhydrolase domain containing 5 (ABHD5), transport to the plasma membrane (not shown), and EOS oxidation catalyzed sequentially by 12R-lipoxygenase, epidermal lipoxygenase 3, and short-chain dehydrogenase/reductase family 9C member 7 (SDR9C7). A subsequent reaction between EOS—epoxy enone (EpO) and peptides of the corneocyte envelope (CE) is thought to occur nonenzymatically to generate protein-bound ω-hydroxy-acyl sphingosine (OS), which may subsequently be hydrolyzed by ceramidases (C'ase) to form bound ω-hydroxy fatty acids (OHFA). **B:** A 53-year—old male ARCI patient with homozygous deletion/in-frame mutations (c.786_788delCTT leading to amino acid loss p. Phe263del) in *ALOX12B*. Note the accentuated skin lines (**black arrow**) and erythroderma that are typical findings in retinoid-treated ARCI. **C—F:** Skin samples from an ARCI-unaffected human subject (**C** and **D**) or from the *ALOX12B*$^{-/-}$ patient (**E** and **F**) were divided and processed for electron microscopy with or without pyridine (Pyr) extraction, as indicated before fixation to extract unbound lipids (osmium post-fix). **D—F:** Covalently bound CLEs were visualized in the Pyr-extracted, ARCI-unaffected sample (**D**), whereas CLEs in the *ALOX12B*$^{-/-}$ sample seemed to be unbound because they were removed by Pyr extraction (**E** and **F**). **G:** Quantification of CLE abundance. **Black arrowheads** indicate CEs; **white arrowheads**, CLEs; **white arrows,** corneodesmosomes (shown to demonstrate that images are in focus). Data show the means ± SEM (**G**). $n = 10$ randomly acquired high-powered fields used for quantification in each determination (**G**). *$P < 0.05$, ***$P < 0.001$. Scale bars = 100 nm (**C—F**). C, corneocyte; C18:2-TAG, linoleoyl triacylglycerol; EpOH, epoxy alcohol; OOH, hydroperoxide.

preparations. The thickness of lipid membranes was quantified digitally using DigitalMicrograph version 3.10.0 (Gatan Inc., Pleasanton, CA) to measure the width of the electron lucent band between (but not including) the surrounding electron dense regions. Distances were calibrated using catalase crystals and a diffraction grating replica. Five widths were determined for each membrane, and five different membranes from at least two high-magnification fields were analyzed from each sample, resulting in 25 measurements for each width determination. CLE abundance and membrane thickness measurements were each done in a single session by an individual (J.M.M.) who was blinded to the sample identities, and all of the images from different samples were mixed together and analyzed in a random order.

Statistical Analysis

Differences between groups of images (each from a single subject or animal) were analyzed for significance using *t*-tests (unpaired, two tailed), and the data are expressed as the means ± SEM.

Results

The ARCI patient who participated in this study was a 53-year—old (at the time of tissue collection) man with a life-long history of ichthyosis (Figure 1B and Supplemental Figure S2). Genetic sequencing identified homozygous deletion/in-frame mutations (c.786_788delCTT leading to
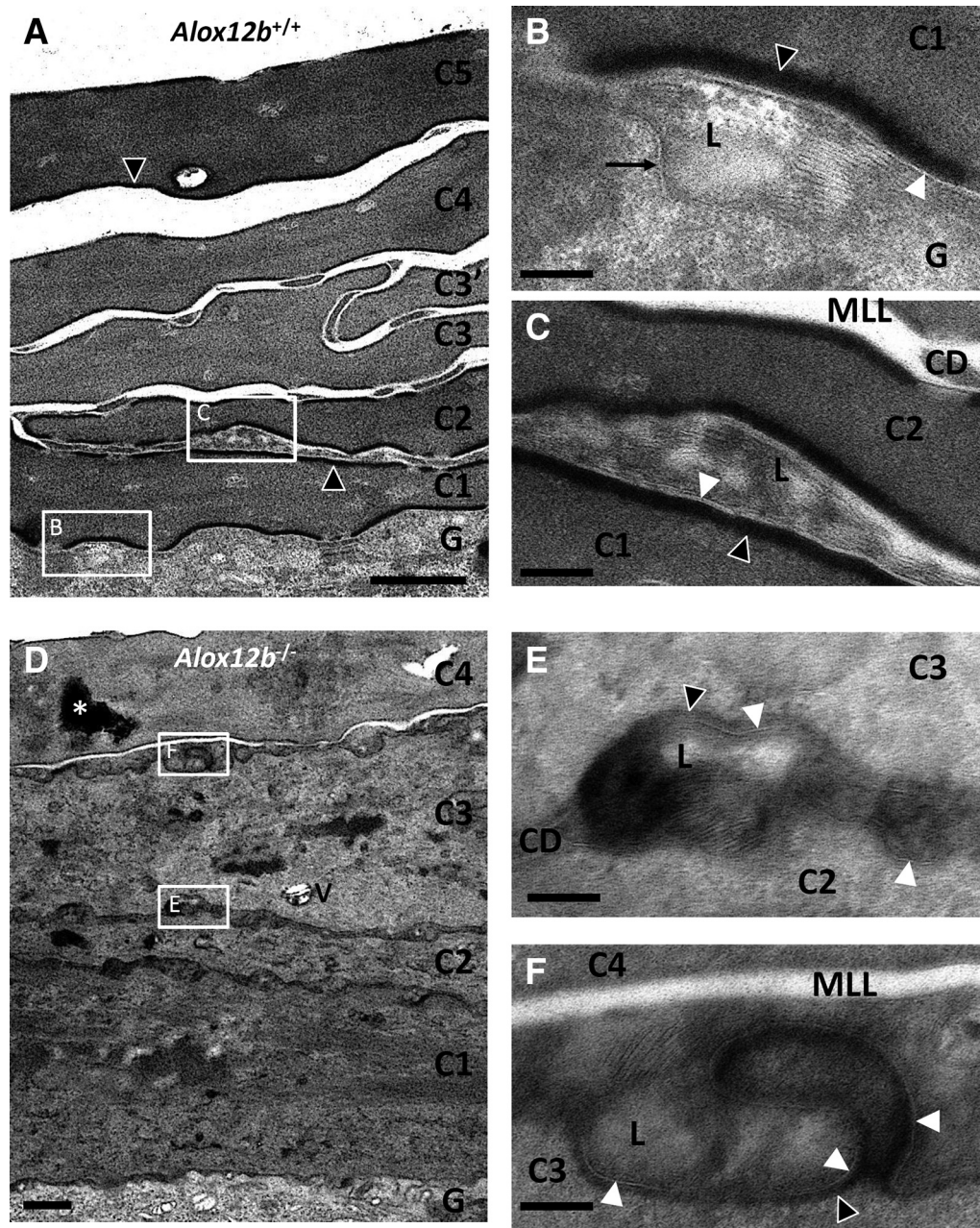
Figure 2 12R-lipoxygenase is required for extracellular lipid processing but not corneocyte lipid envelope (CLE) delivery. **A:** Control stratum corneum (SC) from an *Alox12b*$^{+/+}$ mouse (osmium post-fix) contained corneocytes with homogeneous, electron-dense cytoplasm bounded by conspicuous corneocyte envelopes (CEs). **B** and **C:** Areas outlined by **white boxes** in **A** are shown at higher magnification. **B:** At the stratum granulosum (SG)—SC junction, lipid secretion was observed, composed of stacks of short lipid lamellae mixed with electron-lucent regions, bounded by a lipid membrane on the basal face and a CLE on the apical face. **C:** Above the first SC layer, further lipid processing was observed as secreted lipid lamellae transformed into extended sheets. At more superficial SC levels, interstices between corneocytes were composed mainly of homogeneous electron-lucent spaces that corresponded to mature lipid lamellae (MLL) in ruthenium post-fixed samples (Figure 3A). **D:** In contrast, *Alox12b*$^{-/-}$ SC contained corneocytes with heterogeneous cytoplasm, keratohyalin-like deposits, and electron-lucent vesicular spaces. Lipid secretion appeared normal at the SC-SG junction (not shown). **E** and **F:** Areas outlined by **white boxes** in **D** are shown at higher magnification, showing that interstices at more superficial levels of the SC were surrounded by CLEs and thin CEs, but the lamellar lipids remained in narrow stacks, indicating little or no post-secretory lipid processing. **Asterisk** indicates keratohyalin granule; **black arrow**, lipid membrane; **black arrowheads**, CEs; **white arrowheads**, CLEs. Scale bars: 1 μm (**A** and **D**); 100 nm (**B**, **C**, **E**, and **F**). C1, corneocyte 1; C2, corneocyte 2; C3, corneocyte 3; C3′, corneocyte 3′; C4, corneocyte 4; C5, corneocyte 5; CD, corneodesmosome; G, granular layer keratinocyte; L, lipid deposit; V, vesicular structure.

amino acid loss p. Phe263del) in *ALOX12B* (the gene encoding 12R-LOX). Loss-of-function mutations in *ALOX12B* are one of the most common causes of ARCI.[23] The patient's variant (*rs1302782570*) was only listed once in the Genome Aggregation Database (frequency, 4×10^{-6}), and therefore does not represent a common polymorphism. Prediction programs indicated that the mutation is most likely pathogenic. MutationTaster rated it as
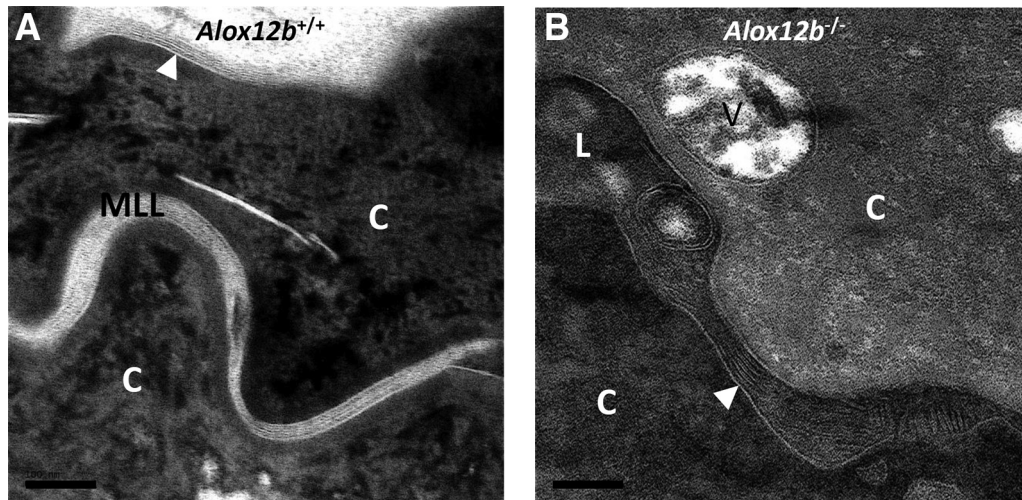
Figure 3 12R-lipoxygenase is required for formation of mature lipid lamellae (MLL) but not corneocyte lipid envelopes (CLEs). Epidermis from *Alox12b*^{+/+} or *Alox12b*^{−/−} mice was processed with ruthenium post-fix to more clearly define the MLL, as reported.[22] **A:** MLL filled most of the stratum corneum (SC) interstices in *Alox12b*^{+/+} mice, among which distinct CLEs could sometimes be identified. **B:** The SC interstices in *Alox12b*^{−/−} mice were surrounded by clearly defined CLEs and filled with incompletely processed lamellar lipids. **White arrowheads** indicate CLEs. Scale bars = 100 nm (**A** and **B**). C, corneocyte; L, lipid deposit; V, vesicular structure.

disease causing (combined annotation dependent depletion, 22.7; <1% top deleterious). The Protein Variation Effect Analyzer score, which predicts whether the insertion/deletion has an impact on the biological function of the protein, was −15.344 (deleterious, cutoff −2.5). The affected residue Phe263 is conserved between human, mouse, and dog, and lies at the beginning of the lipoxygenase catalytic domain. A similar deletion mutation in *ALOX12B* (c.787_789delTTC, p. Phe262del, also a highly conserved residue) was recently reported in a compound heterozygous ARCI patient from the Czech Republic.[24] The patient in the current study had been taking oral retinoids continuously for >30 years, which helped to control scale but left him with persistent erythroderma, suggesting that the retinoids did not address the underlying functional defect. A skin specimen was obtained for further evaluation by electron microscopy.

If 12R-LOX specifically contributes to CLE-CE cross-linking, *ALOX12B*^{−/−} SC could contain unbound CLEs (eg, lipid membranes attached to CEs only by noncovalent interactions), but these have not been reported. Such unbound CLEs should be extracted by treatment with organic solvents. Pyridine has been shown to extract unbound SC lipids to an extent comparable to chloroform/methanol solutions, while preventing fusion of adjacent CLEs to enhance visualization.[25] Indeed, CLEs were readily identified in unextracted SC from the *ALOX12B*^{−/−} ARCI patient (Figure 1E), but not in the pyridine-extracted sample (Figure 1F). Quantification showed that the CLEs were 81% (*P* = 0.035) less abundant in the pyridine-extracted sample compared with the unextracted sample (Figure 1G). These CLEs were associated with incomplete processing of secreted lipids (not shown, but consistent with findings in *Alox12b*^{−/−} mice, as described below). In contrast, in

control SC (from normal appearing skin from an ARCI-unaffected human subject), CLEs were almost exclusively visible in pyridine-extracted samples (Figure 1, C and D); quantification is shown (Figure 1G), as reported.[1] The abundance of CLEs in unextracted *ALOX12B*^{−/−} SC was similar to that in pyridine-extracted control SC, suggesting that 12R-LOX is not required for CLE formation per se. However, the evidence that CLEs are not covalently bound in *ALOX12B*^{−/−} SC indicates that 12R-LOX plays an essential role in CLE-CE cross-linking.

To investigate this observation with better experimental controls (age- and sex-matched wild-type samples processed in parallel), epidermis from *Alox12b* conditional knockout mice (*Alox12b*^{−/−}) was examined in comparison to control mice lacking the causes recombination recombinase transgene (*Alox12b*^{+/+}). These samples were obtained during a previously published study in which *Alox12b* gene deletion in epidermal keratinocytes was confirmed.[19] Similar to the ARCI patient with mutations in *ALOX12B*, unextracted samples from *Alox12b*^{−/−} mice contained abundant CLEs at all levels of the SC (Figure 2, D−F, and Figure 3B), but these CLEs were extracted by treatment with pyridine (Figure 4, B and D); quantification is shown (Figure 5A). The unbound CLEs in *Alox12b*^{−/−} SC surrounded secreted lipid lamellae that failed to be processed into mature lipid lamellae, unlike *Alox12b*^{+/+} SC, where bound CLEs were present in the first SC layer (Figure 4A) as well as in more superficial SC levels (Figure 4C), and lipid processing was almost always completed above the second SC layer (Figures 2, A−C, and 3A). Although most of the interstices contained no lipid deposits in pyridine-extracted *Alox12b*^{−/−} SC, a few contained lipid membranes that appeared to be partially attached or tethered to the CE (Figure 4D). These
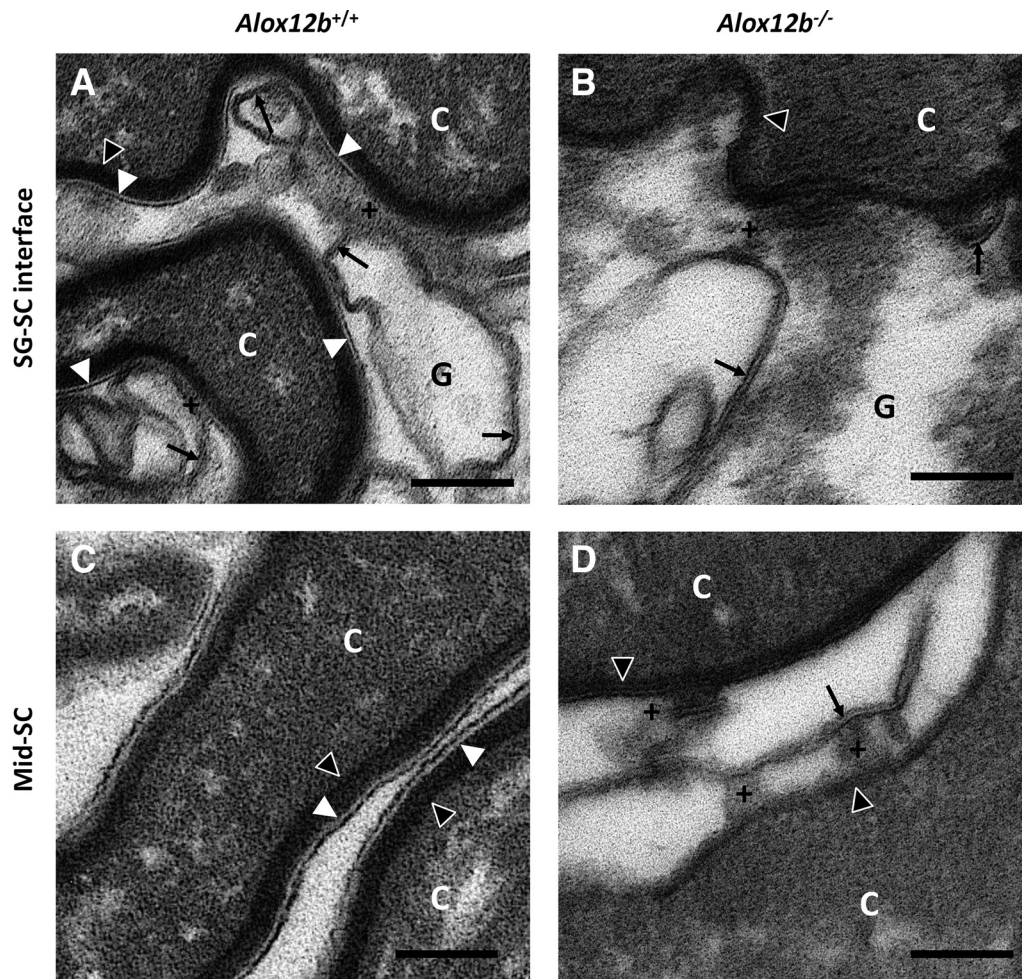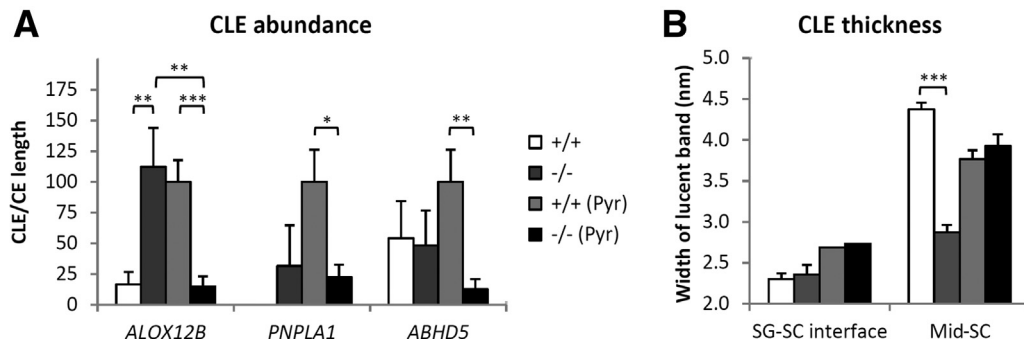
Figure 4 12R-lipoxygenase deficiency impairs corneocyte lipid envelope (CLE)—corneocyte envelope (CE) cross-linking and is associated with partially attached lipid membranes. Epidermis from $Alox12b^{+/+}$ or $Alox12b^{-/-}$ mice was extracted with pyridine to remove unbound lipids and processed for electron microscopy (osmium post-fix). Bound CLEs were abundant only in $Alox12b^{+/+}$ samples and were thinner at the stratum granulosum (SG)—stratum corneum (SC) interface (**A**) compared with the mid-SC (**C**). In contrast, CE thickness did not appear to differ between these locations. Whorled lipid membranes were a constant finding in granular keratinocytes at the SG-SC junction in both $Alox12b^{+/+}$ (**A**) and $Alox12b^{-/-}$ (**B**) pyridine-extracted samples. No bound CLEs were found at the SG-SC interface in $Alox12b^{-/-}$ samples (**B**), and although most of the interstices in the $Alox12b^{-/-}$ SC contained no visible lipid (not shown), a few contained lipid membranes (**D**) that resembled the whorled membranes at the SG-SG junction, in some cases appearing to be partially attached or tethered to the nearby CEs. **Black arrows** indicate lipid membranes; **black arrowheads**, CEs; **plus sign**, electron-dense material apparently tethering a lipid membrane to a CE; **white arrowheads**, CLEs. Scale bars = 100 nm (**A**–**D**). +, Electron-dense material apparently tethering a lipid membrane to a CE; C, corneocyte; G, granular layer keratinocyte.

tethered membranes resembled whorled lipid membranes that were a constant finding at the stratum granulosum—SC interface in both $Alox12b^{+/+}$ and $Alox12b^{-/-}$ pyridine-extracted epidermis (Figure 4, A and B) and could represent immature CLEs and/or residual lamellar lipids not extracted by pyridine. $Alox12b^{-/-}$ SC also featured attenuated CEs and heterogeneous corneocyte cytoplasm containing retained keratohyalin granules and lipid vesicles, as reported.[20]

To determine whether unbound CLEs are specific to 12R-LOX deficiency, CLE abundance was quantified in $Alox12b^{-/-}$ SC in comparison to SC from $Pnpla1^{-/-}$ or $Abhd5^{-/-}$ mice that have defective EOS synthesis (Figure 5A). Samples were obtained during previously

published studies in which deletion of the indicated gene was confirmed.[11,19,21] As previously reported in these studies, there was a significant decrease in CLE abundance in pyridine-extracted samples in knockout versus wild-type mice in all three mouse models, but only $Alox12b^{-/-}$ samples showed abundant unbound CLEs (ie, significantly greater abundance of CLEs in unextracted compared with pyridine-extracted SC).

To further evaluate the role of 12R-LOX in CLE formation, CLE thickness was quantified in $Alox12b^{+/+}$ versus $Alox12b^{-/-}$ SC (Figure 5B). In the mid-SC, the average thickness of $Alox12b^{+/+}$ CLEs (4.37 ± 0.12 and 3.76 ± 0.12 nm in unextracted and extracted samples, respectively) as well as the bound CLEs in extracted

Figure 5 Unbound corneocyte lipid envelopes (CLEs) are specific to 12R-lipoxygenase deficiency and have thicknesses similar to immature CLEs. **A** and **B:** Epidermis from the indicated [+/+] or [-/-] mice (**A**) or from *Alox12b*^{+/+} or *Alox12b*^{-/-} mice (**B**) were treated with or without pyridine (Pyr), as indicated, to extract unbound lipids, then fixed and processed for electron microscopy (osmium post-fix). **A:** CLE abundance was quantified as the percentage corneocyte envelope (CE) length with associated CLE, normalized to the value obtained with [+/+] (Pyr). **B:** The thickness of CLEs at the indicated location [stratum granulosum (SG)−stratum corneum (SC) interface or mid-SC] was quantified as the diameter of lucent bands. Additional statistical analyses are given in the main text. Data are presented as means ± SEM (**A** and **B**). $n = 10$ random high-magnification images from 1 mouse (**A**); $n = 25$ measurements of 4 distinct structures from 1 mouse each (**B**). *$P < 0.05$, **$P < 0.01$, and ***$P < 0.001$.

*Alox12b*^{-/-} samples (3.93 ± 0.31 nm; note that these were less abundant, as shown) (Figure 5A) were similar to previous determinations of CLE thickness at approximately 4 nm.[2,26] In comparison, the unbound CLEs and partially tethered lipid membranes (Figure 4D) in *Alox12b*^{-/-} SC were significantly thinner (2.87 ± 0.09 and 3.01 ± 0.12 nm, respectively). These differences were only found in mature CLEs, because the thickness of incipient CLEs at the stratum granulosum−SC interface and the membranes surrounding lamellar bodies (Supplemental Figure S3) did not differ between *Alox12b*^{+/+} and *Alox12b*^{-/-}.

Discussion

The major novel finding of this study is that an abnormal type of CLE is present in *ALOX12B*^{-/-} and *Alox12b*^{-/-} SC, but not in SC from normal human or mouse skin or from mice with deletion of genes involved in EOS synthesis (*Pnpla1* or its cofactor *Abhd5/Cgi-58*). Because treatment with pyridine (shown to extract free lipids from epidermal samples to a degree similar to chloroform/methanol mixtures[25]) greatly reduced the abundance of CLEs in *ALOX12B*^{-/-} and *Alox12b*^{-/-} SC, these abnormal CLEs are not covalently

bound to the CE, and instead maintain contact via noncovalent interactions. Matched control samples show the opposite change with pyridine treatment, so these effects are unlikely to be due to a processing artifact. The unbound CLEs are thinner than normal mature CLEs and are associated with failure to process secreted lipids into mature lipid lamellae.

These observations help to clarify the function of 12R-LOX in the context of CLE formation and maturation. Similar to previous reports,[14,27] 12R-LOX was found in the current study to be required for most CLE-CE cross-linking. However, this is the first report that CLE formation occurs independently of 12R-LOX−dependent CLE-CE cross-linking. This is consistent with the recent proposal[5] that the CLE derives from the limiting membrane of lamellar bodies during lipid secretion, because the latter are normal in *Alox12b*^{-/-} epidermis (Supplemental Figure S3). On the other hand, the 12R-LOX−dependent cross-linking step appears to be essential for CLE maturation (eg, development into the final 4-nm−thick membrane) and for its proposed function in lamellar lipid processing. Together, these results support a specific role for 12R-LOX in CLE-CE cross-linking, as proposed in the current model of CLE biogenesis (Figure 1A).
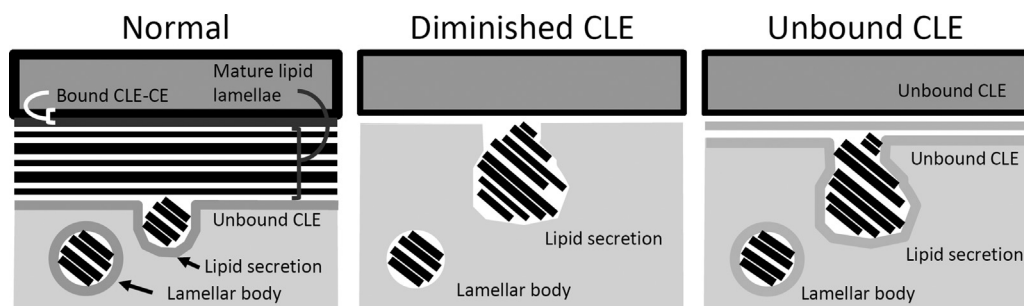
Figure 6 Models illustrating effective lipid processing in the context of a normal, covalently bound corneocyte lipid envelope (CLE), in comparison with defective lipid processing associated with a diminished CLE and an unbound CLE. Structures are not to scale. CE, corneocyte envelope.

One limitation of this study is that it was not possible to determine the composition of the thin, unbound CLEs in $Alox12b^{-/-}$ SC. Lipid analysis on these mice was previously published,[19] showing that $Alox12b^{-/-}$ epidermis contained increased EOS compared with $Alox12b^{+/+}$, similar to an independent report in constitutive 12R-LOX knockout mice.[20] EOS is thought to be the major precursor of covalently bound ω-hydroxy-acyl sphingosine, so it is tempting to speculate that the unbound CLEs contain EOS. However, this could not be confirmed, because the lipids of the unbound CLEs mix with other free extractable lipids during lipid extraction, making them indistinguishable. Because CLEs at the stratum granulosum–SC junction are thinner than CLEs in the mid-SC, there appears to be a maturation period in which the composition and/or molecular orientation of lipids within the CLE change. CLE-CE cross-linking might be expected to reduce molecular mobility, making lipid chain packing tighter and resulting in a thicker and more rigid membrane, but further studies are needed to characterize the composition, structure, and function of free versus covalently bound CLEs.

On the basis of these findings, CLE dysfunction can be caused by at least two distinct structural defects (Figure 6): diminished CLEs and unbound CLEs. Diminished CLEs can result from inadequate EOS synthesis, caused by genetic mutations and/or reduced expression or activity of enzymes involved in EOS synthesis, or increased activity of ceramidases that degrade EOS and other ceramides.[17] This type of CLE can be identified by the presence of attenuated lamellar body limiting membranes and CLEs. In contrast, unbound CLEs are a feature of 12R-LOX deficiency, in which EOS synthesis is normal,[20] but CLE-CE cross-linking is defective. Unbound CLEs can be detected by comparing CLEs in pyridine-extracted versus unextracted samples, as shown herein. $ALOXE3^{-/-}$ and $SDR9C7^{-/-}$ SC may also contain unbound CLEs, although these conditions were not examined in the current study. Reduced abundance of 12R-LOX substrates (eg, reduced linoleic acid–containing EOS in essential fatty acid deficiency[28] and within comedones of acne vulgaris[29]) could also result in unbound CLEs despite adequate 12R-LOX protein expression. The proposed role of 12R-LOX in CLE biogenesis and the distinction between diminished and unbound CLEs should be considered in the development of therapies for ARCI and other conditions.

Acknowledgments

Supplemental Data

Supplemental material for this article can be found at http://doi.org/10.1016/j.ajpath.2021.02.005.

Author Contributions

J.M.M., H.S., M.S., F.P.W.R., S.G., T.M.M., and P.M.E. did conceptualization; J.M.M. and D.C. performed data curation; J.M.M. performed formal analysis; T.M.M. and P.M.E. acquired funding; J.M.M., D.C., H.S., A.D., M.S., R.G., F.P.W.R., and S.G. conducted the investigation; J.M.M., D.C., H.S., A.D., F.P.W.R., S.G., and P.M.E. developed the methodology; J.M.M., H.S., A.D., M.S., R.G., F.P.W.R., S.G., T.M.M., and P.M.E. performed project administration; H.S., A.D., M.S., R.G., F.P.W.R., and S.G. acquired resources; J.M.M. and J.S.W. performed visualization; J.M.M. wrote the original manuscript; M.S., F.P.W.R., S.G., J.S.W., T.M.M., and P.M.E. reviewed and edited the manuscript.

References

1. Elias PM, Goerke J, Friend DS: Mammalian epidermal barrier layer lipids: composition and influence on structure. J Invest Dermatol 1977, 69:535–546
2. Swartzendruber DC, Wertz PW, Madison KC, Downing DT: Evidence that the corneocyte has a chemically bound lipid envelope. J Invest Dermatol 1987, 88:709–713
3. Elias PM, Schmuth M, Uchida Y, Rice RH, Behne M, Crumrine D, Feingold KR, Holleran WM: Basis for the permeability barrier abnormality in lamellar ichthyosis. Exp Dermatol 2002, 11:248–256
4. Akiyama M: Corneocyte lipid envelope (CLE), the key structure for skin barrier function and ichthyosis pathogenesis. J Dermatol Sci 2017, 88:3–9
5. Crumrine D, Khnykin D, Krieg P, Man MQ, Celli A, Mauro TM, Wakefield JS, Menon G, Mauldin E, Miner JH, Lin MH, Brash AR, Sprecher E, Radner FPW, Choate K, Roop D, Uchida Y, Gruber R, Schmuth M, Elias PM: Mutations in recessive congenital ichthyoses illuminate the origin and functions of the corneocyte lipid envelope. J Invest Dermatol 2019, 139:760–768
6. Hohl D, Huber M, Frenk E: Analysis of the cornified cell envelope in lamellar ichthyosis. Arch Dermatol 1993, 129:618–624
7. Macheleidt O, Kaiser HW, Sandhoff K: Deficiency of epidermal protein-bound omega-hydroxyceramides in atopic dermatitis. J Invest Dermatol 2002, 119:166–173
8. Wertz PW, Swartzendruber DC, Kitko DJ, Madison KC, Downing DT: The role of the corneocyte lipid envelope in cohesion of the stratum corneum. J Invest Dermatol 1989, 93:169–172
9. Ohno Y, Kamiyama N, Nakamichi S, Kihara A: PNPLA1 is a trans-acylase essential for the generation of the skin barrier lipid omega-O-acylceramide. Nat Commun 2017, 8:14610
10. Ohno Y, Nara A, Nakamichi S, Kihara A: Molecular mechanism of the ichthyosis pathology of Chanarin-Dorfman syndrome: stimulation of PNPLA1-catalyzed omega-O-acylceramide production by ABHD5. J Dermatol Sci 2018, 92:245–253
11. Kien B, Grond S, Haemmerle G, Lass A, Eichmann TO, Radner FPW: ABHD5 stimulates PNPLA1-mediated omega-O-acylceramide biosynthesis essential for a functional skin permeability barrier. J Lipid Res 2018, 59:2360–2367
12. Grayson S, Johnson-Winegar AG, Wintroub BU, Isseroff RR, Epstein EH Jr, Elias PM: Lamellar body-enriched fractions from neonatal mice: preparative techniques and partial characterization. J Invest Dermatol 1985, 85:289–294
13. Sevilla LM, Nachat R, Groot KR, Klement JF, Uitto J, Djian P, Maatta A, Watt FM: Mice deficient in involucrin, envoplakin, and periplakin have a defective epidermal barrier. J Cell Biol 2007, 179:1599–1612

14. Zheng Y, Yin H, Boeglin WE, Elias PM, Crumrine D, Beier DR, Brash AR: Lipoxygenases mediate the effect of essential fatty acid in skin barrier formation: a proposed role in releasing omega-hydroxyceramide for construction of the corneocyte lipid envelope. J Biol Chem 2011, 286:24046−24056

15. Takeichi T, Hirabayashi T, Miyasaka Y, Kawamoto A, Okuno Y, Taguchi S, Tanahashi K, Murase C, Takama H, Tanaka K, Boeglin WE, Calcutt MW, Watanabe D, Kono M, Muro Y, Ishikawa J, Ohno T, Brash AR, Akiyama M: SDR9C7 catalyzes critical dehydrogenation of acylceramides for skin barrier formation. J Clin Invest 2020, 130:890−903

16. Hirabayashi T, Anjo T, Kaneko A, Senoo Y, Shibata A, Takama H, Yokoyama K, Nishito Y, Ono T, Taya C, Muramatsu K, Fukami K, Munoz-Garcia A, Brash AR, Ikeda K, Arita M, Akiyama M, Murakami M: PNPLA1 has a crucial role in skin barrier function by directing acylceramide biosynthesis. Nat Commun 2017, 8:14609

17. Kihara A: Synthesis and degradation pathways, functions, and pathology of ceramides and epidermal acylceramides. Prog Lipid Res 2016, 63:50−69

18. Oji V, Tadini G, Akiyama M, Blanchet Bardon C, Bodemer C, Bourrat E, et al: Revised nomenclature and classification of inherited ichthyoses: results of the First Ichthyosis Consensus Conference in Soreze 2009. J Am Acad Dermatol 2010, 63:607−641

19. Krieg P, Dick A, Latzko S, Rosenberger S, Meyer J, Crumrine D, Hielscher T, Elias PM, Rauh M, Schneider H: Conditional Alox12b knockout: degradation of the corneocyte lipid envelope in a mouse model of autosomal recessive congenital ichthyoses. J Invest Dermatol 2020, 140:249−253.e6

20. Epp N, Furstenberger G, Muller K, de Juanes S, Leitges M, Hausser I, Thieme F, Liebisch G, Schmitz G, Krieg P: 12R-lipoxygenase deficiency disrupts epidermal barrier function. J Cell Biol 2007, 177:173−182

21. Grond S, Eichmann TO, Dubrac S, Kolb D, Schmuth M, Fischer J, Crumrine D, Elias PM, Haemmerle G, Zechner R, Lass A, Radner FP: PNPLA1 deficiency in mice and humans leads to a defect in the synthesis of omega-O-acylceramides. J Invest Dermatol 2017, 137:394−402

22. Hou SY, Mitra AK, White SH, Menon GK, Ghadially R, Elias PM: Membrane structures in normal and essential fatty acid-deficient stratum corneum: characterization by ruthenium tetroxide staining and x-ray diffraction. J Invest Dermatol 1991, 96:215−223

23. Eckl KM, de Juanes S, Kurtenbach J, Natebus M, Lugassy J, Oji V, Traupe H, Preil ML, Martinez F, Smolle J, Harel A, Krieg P, Sprecher E, Hennies HC: Molecular analysis of 250 patients with autosomal recessive congenital ichthyosis: evidence for mutation hotspots in ALOXE3 and allelic heterogeneity in ALOX12B. J Invest Dermatol 2009, 129:1421−1428

24. Buckova H, Noskova H, Borska R, Reblova K, Pinkova B, Zapletalova E, Kopeckova L, Horky O, Nemeckova J, Gaillyova R, Nagy Z, Vesely K, Hermanova M, Stehlikova K, Fajkusova L: Autosomal recessive congenital ichthyoses in the Czech Republic. Br J Dermatol 2016, 174:405−407

25. Elias PM, Fartasch M, Crumrine D, Behne M, Uchida Y, Holleran WM: Origin of the corneocyte lipid envelope (CLE): observations in harlequin ichthyosis and cultured human keratinocytes. J Invest Dermatol 2000, 115:765−769

26. Lavker RM: Membrane coating granules: the fate of the discharged lamellae. J Ultrastruct Res 1976, 55:79−86

27. Dick A, Tantcheva-Poor I, Oji V, Giehl KA, Fischer J, Krieg P, Schneider H, Rauh M: Diminished protein-bound omega-hydroxylated ceramides in the skin of patients with ichthyosis with 12R-lipoxygenase (LOX) or eLOX-3 deficiency. Br J Dermatol 2017, 177: e119−e121

28. Wertz PW, Cho ES, Downing DT: Effect of essential fatty acid deficiency on the epidermal sphingolipids of the rat. Biochim Biophys Acta 1983, 753:350−355

29. Perisho K, Wertz PW, Madison KC, Stewart ME, Downing DT: Fatty acids of acylceramides from comedones and from the skin surface of acne patients and control subjects. J Invest Dermatol 1988, 90:350−353